Available online at www.sciencedirect.com

ScienceDirect

IFAC PapersOnline CONFERENCE PAPER ARCHIVE

IFAC PapersOnLine 52-5 (2019) 378–384

Linear Time-Variant Vehicle Trajectory Guidance with Nonlinear Inversion-Based Feedforward Control ⋆

J. Schucker * **U. Konigorski** **

* *Opel Automobile GmbH, Bahnhofsplatz, 65432 Ruesselsheim am Main, Germany (e-mail: jeremias.schucker@opel.com).*
** *Department of Control Systems and Mechatronics, Technical University Darmstadt, Landgraf-Georg-Str. 4, 64283 Darmstadt, Germany (e-mail: ukonigorski@iat.tu-darmstadt.de)*

Abstract: This work presents a two-degree-of-freedom (2DOF) control concept for vehicle trajectory guidance for automated driving on highways consisting of a nonlinear feedforward control and a linear time-variant feedback controller. To obtain a linear time-variant system of the error dynamics the nonlinear vehicle model is linearized along a given trajectory. To relieve the feedback controller future knowledge of the vehicle movement contained in the trajectory is used to create a nonlinear inversion-based feedforward control. Finally, the control concept is applied in a sophisticated simulation environment and compared to a nonlinear benchmark controller. In addition, model states are chosen in a way that all required signals can be obtained by state-of-the-art hardware of production vehicles.

Keywords: Time-variant control, feedforward control, system inversion, automated guided vehicles, linear quadratic regulator

1. INTRODUCTION

Advanced driver assistance systems (ADAS) are getting more and more in focus as the demand for automated vehicles grows. The task of current ADAS such as e. g. adaptive cruise control or lane keeping/centering systems is basically to keep the vehicle within the lane or to set a desired velocity. For automated driving, though, this is not sufficient. In order to e. g. automatically enter a highway it is necessary for a vehicle to precisely follow a planned trajectory. Vehicle trajectory guidance has already been intensively studied in literature. Linear control concepts do neglect the fact that the vehicle dynamics changes significantly especially for different velocities. Therefore, it is necessary to design a set of controllers for different operating points (Schorn and Isermann, 2006) or consider the vehicle speed as time-variant parameter (Ballesteros-Tolosana et al., 2017). In addition, there is a huge variety of powerful nonlinear control concepts. Differential geometric control methods such as feedback linearization (Freund and Mayr, 1997) or (Schucker and Konigorski, 2018) achieve great tracking performance on the cost of a rather complex control law. Werling et al. (2010) propose a Lyapunov tracking controller but there is no general approach to obtain a Lyapunov control law. Conventional model predictive controllers (MPC) are computationally expensive and generally cannot cope with unknown disturbances (Bahadorian et al., 2014). On the other hand, creating a time-variant model by linearizing the nonlinear model around a trajectory makes it possible to use the best-suited properties of both linear and nonlinear control. I.e. a model that precisely describes the current dynamics as long as the vehicle is close to the planned trajectory and to use a simple 'linear' control law. Time-variant control is often ignored in practical applications (Thimmaraya et al., 2010). Nevertheless, it has been applied to aerial vehicles (Thimmaraya et al., 2010) though this approach requires the solution of a differential Sylvester equation. By Miah et al. (2017) and Bahadorian et al. (2014) time-variant control is applied for mobile robots but both need an online solution of an optimal control problem. In this paper, a two-degree-of-freedom control concept is introduced. It consists of an inversion-based feedforward control using the nonlinear model. To handle disturbances and model uncertainties an optimal time-variant controller is designed based on a linear quadratic cost function. The control law is a simple time-variant state feedback which is obtained by solving the optimal control problem via backward integration. Thus, the control concept overcomes the described shortages, i. e. the controller

- uses an exact model and, thus, is valid over the whole operation range,
- has a simple control law, and
- can easily be calculated online.

The rest of this work is organized as follows: The nonlinear vehicle model is introduced in Section 2. Subsequently, the inversion-based feedforward controller is presented followed by the time-variant controller design. Section 4 shortly introduces the benchmark controller and gives a

⋆ This work results from the joint project 'Ko-HAF - Cooperative Highly Automated Driving' and has been funded by the Federal Ministry for Economic Affairs and Energy based on a resolution of the German Bundestag.

10.1016/j.ifacol.2019.09.061

short conceptual comparison to the time-variant control concept. Eventually, the experimental setup and results are described in Section 5 and conclusions are drawn in Section 6.

2. SYSTEM MODEL

This section provides a complete vehicle model of a prototype vehicle, an Opel Insignia Sports Tourer (automatic transmission, 184 kW power, four-wheel drive). It consists of a nonlinear vehicle model and linear actuator dynamics. It also contains the main characteristic of the street, the curvature $\kappa(t)$, as time-variant parameter.

2.1 Horizontal Vehicle Dynamics

Vehicle dynamics has widely been discussed in literature (e. g. Rajamani (2012)). Most commonly used for controller design is a single-track model firstly introduced by Riekert and Schunk (1940). The three basic kinetic equations of the single-track model are

$$\ddot{\psi} = \frac{-F_{y\mathrm{r}} l_\mathrm{r} + F_{y\mathrm{f}} l_\mathrm{f} \cos(\delta) + F_{x\mathrm{f}} l_\mathrm{f} \sin(\delta)}{I_\mathrm{z}} \tag{1}$$

$$\dot{\beta} = -\dot{\psi} + \frac{F_{y\mathrm{f}} \cos(\delta-\beta) + F_{x\mathrm{f}} \sin(\delta-\beta)}{mv} + \cdots$$
$$\cdots + \frac{F_{y\mathrm{r}} \cos(\beta) - F_{x\mathrm{r}} \sin(\beta)}{mv} \tag{2}$$

$$\dot{v} = \frac{-F_{y\mathrm{f}} \sin(\delta-\beta) + F_{x\mathrm{f}} \cos(\delta-\beta)}{m} + \cdots$$
$$\cdots + \frac{F_{y\mathrm{r}} \sin(\beta) + F_{x\mathrm{r}} \cos(\beta)}{m}, \tag{3}$$

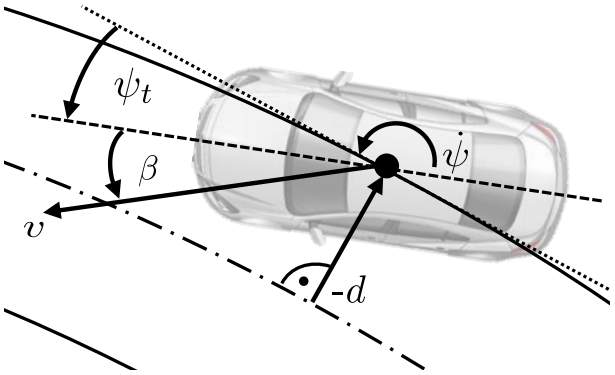

Fig. 1. Vehicle model, —— lane boundaries, —·— lane center line, ····· tangent to the road, - - - - vehicle longitudinal axis

where yaw rate $\dot{\psi}$, side slip angle β, and velocity v are the three vehicle dynamics states. $F_{x\mathrm{f}}$ and $F_{x\mathrm{r}}$ are the longitudinal wheel forces at front and rear axle respectively. They can be expressed in terms of a general longitudinal force F_x via the following expression $F_{x\mathrm{f}} = \mu F_x$ and $F_{x\mathrm{r}} = (1-\mu)F_x$. δ is the steering angle at the front wheels. $F_{y\mathrm{f}}$ and $F_{y\mathrm{r}}$ are lateral tire forces calculated by using a linear tire model (Rajamani, 2012). The usage of a linear tire model is sufficient since only maneuvers with rather low dynamics and, thus, with small tire slip angles are considered. To guide a vehicle along a trajectory on a road the lateral offset to the lane center is necessary. In longitudinal direction it is sufficient to set a proper speed. The exact position along the road does not matter. Hence, two more states are added to the model to describe the vehicle motion along the road. The two states are the lateral distance from the lane center d and a street-relative yaw angle ψ_t as depicted Fig. 1. The differential equations for the newly introduced states are

$$\dot{d} = v \sin(\psi_\mathrm{t} + \beta) \tag{4}$$

$$\dot{\psi}_\mathrm{t} = \dot{\psi} - v \cos(\psi_\mathrm{t} + \beta)\kappa(t), \tag{5}$$

where $v\sin(\psi_\mathrm{t}+\beta)$ describes the speed orthogonal and $v\cos(\psi_\mathrm{t}+\beta)$ tangential to the current lane center. $\kappa(t)$ is a time-varying parameter and describes the curvature of the street. Finally, the vehicle dynamics model can be written as

$$\dot{\bar{\mathbf{x}}} = \bar{\mathbf{f}}\big(\bar{\mathbf{x}}, \kappa(t), \bar{\mathbf{u}}\big) \tag{6}$$

with $\bar{\mathbf{x}} = [d \;\; \psi_\mathrm{t} \;\; \dot{\psi} \;\; \beta \;\; v]'$, $\bar{\mathbf{u}} = [\delta \;\; F_x]'$
where the apostrophe (') denotes the transpose.

2.2 Full Vehicle Model

As shown by Schucker and Konigorski (2018) precise tracking of a reference trajectory requires to consider actuator dynamics in the vehicle model. Both actuator dynamics i. e. steering dynamics and longitudinal (engine/brake) dynamics can be modeled as second-order linear systems. Putting the longitudinal and steering dynamics together with the vehicle dynamics model (6), a full vehicle model is obtained:

$$\underbrace{\frac{\mathrm{d}}{\mathrm{d}t}\begin{bmatrix}\bar{\mathbf{x}}\\ \delta\\ \dot{\delta}\\ F_x\\ \dot{F}_x\end{bmatrix}}_{\dot{\mathbf{x}}} = \underbrace{\begin{bmatrix}\bar{\mathbf{f}}(\bar{\mathbf{x}}, \kappa(t), \bar{\mathbf{u}})\\ \dot{\delta}\\ -2D_\mathrm{s}\omega_\mathrm{s}\dot{\delta} - \omega_\mathrm{s}^2\delta\\ \dot{F}_x\\ -2D_\mathrm{l}\omega_\mathrm{l}\dot{F}_x - \omega_\mathrm{l}^2 F_x\end{bmatrix}}_{\mathbf{f}(\mathbf{x},\kappa(t))} + \underbrace{\begin{bmatrix}0\\ 0\\ K_\mathrm{s}\omega_\mathrm{s}^2\delta_\mathrm{c}\\ 0\\ K_\mathrm{l}\omega_\mathrm{l}^2 F_{x,\mathrm{c}}\end{bmatrix}}_{\mathbf{g}(\mathbf{x})\mathbf{u}} \tag{7a}$$

$$\mathbf{y} = \mathbf{h}(\mathbf{x}) = [y_1 \;\; y_2] = [v \;\; d]', \tag{7b}$$

with states $\mathbf{x} = [d \;\; \psi_\mathrm{t} \;\; \dot{\psi} \;\; \beta \;\; v \;\; \delta \;\; \dot{\delta} \;\; F_x \;\; \dot{F}_x]'$
and controls $\mathbf{u} = [\delta_\mathrm{c} \;\; F_{x,\mathrm{c}}]'$.

F_x, $\dot{F}_x$ and δ, $\dot{\delta}$ are the states of the actuator dynamics and $F_{x,\mathrm{c}}$ and δ_c are the new inputs of the model. $D_\mathrm{s}, D_\mathrm{l}$ being the damping, $w_\mathrm{s}, w_\mathrm{l}$ the eigen angular frequency and $K_\mathrm{s}, K_\mathrm{l}$ the static gain of the actuator dynamics. In general, in a vehicle the steering angle at the front wheels cannot be measured. However, the front wheels are mechanically connected to the steering wheel. The connection can roughly be assumed to be stiff and velocity independent. Thus, the steering angle at the front wheels δ can be obtained through the steering wheel angle δ_{sw} with

$\delta = \frac{\delta_{\text{sw}}}{i_{\text{sw}}}$ where i_{sw} is the constant steering transmission ratio.

3. CONTROLLER DESIGN

The presented control approach is based on the two-degree-of-freedom structure (Horowitz, 1963) illustrated in Fig. 2 where the variables with an asterisk (*) describe feedforward quantities. The main advantage of a two-degree-of-freedom control is that tracking and disturbance behavior can be adjusted separately. This is an essential property for tracking problems where it is important not only to compensate modeling uncertainties and disturbances but also to precisely follow a given trajectory. In the following first the inversion-based feedforward controller and the time-variant linear quadratic controller (TVLQR) are presented.

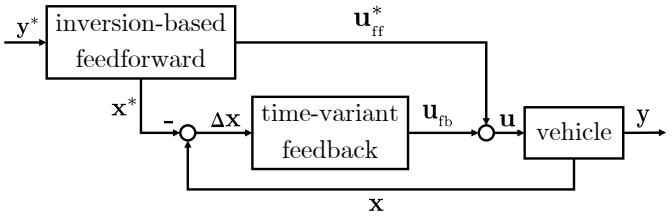

Fig. 2. 2DOF structure containing the inversion-based feedforward and the time-variant feedback control

3.1 Inversion-Based Feedforward Control

Most commonly the desired trajectory $\mathbf{y}^*$ is planned for the output of a system. The task of the feedforward control is to design a desired input $\mathbf{u}_{\text{ff}}^*$ which guides the vehicle along this trajectory by only using the information contained in $\mathbf{y}^*$. Thus, no measurement information is necessary. In the absence of disturbances and modeling uncertainties, $\mathbf{u}_{\text{ff}}^*$ leads to $\boldsymbol{\Delta}\mathbf{y} = \mathbf{y} - \mathbf{y}^* = 0,\ t \geq 0$. In addition to the desired input $\mathbf{u}_{\text{ff}}^*$ the feedforward control also needs to generate the desired states $\mathbf{x}^*$ required for the time-variant controller described in the next section. The feedforward control is based on the Hirschorn Inverse (Hirschorn, 1979). In order to calculate the Hirschorn Inverse the desired state $\mathbf{x}^*$ is used. Hence, a coordinate transformation of the form

$$\mathbf{z}^* = \begin{bmatrix} \boldsymbol{\xi}_1^* \\ \boldsymbol{\xi}_2^* \\ \boldsymbol{\eta}^* \end{bmatrix} = \boldsymbol{\Phi}(\mathbf{x}^*) \tag{8}$$

is required, where $\boldsymbol{\Phi}$ is a diffeomorphism and

$$\boldsymbol{\xi}_1^* = \begin{bmatrix} y_1^* \\ \dot{y}_1^* \\ \ddot{y}_1^* \end{bmatrix}, \quad \boldsymbol{\xi}_2^* = \begin{bmatrix} y_2^* \\ \dot{y}_2^* \\ \ddot{y}_2^* \\ \dddot{y}_2^* \end{bmatrix}, \text{ and } \quad \boldsymbol{\eta}^* = \begin{bmatrix} \eta_1^* \\ \eta_2^* \end{bmatrix}. \tag{9}$$

$\boldsymbol{\xi}_1^*$ and $\boldsymbol{\xi}_2^*$ have the dimension of the relative degree of their corresponding output. For the presented model (Eq. 7) the relative degrees are $[r_1\ r_2] = [3\ 4]$. $\boldsymbol{\eta}^*$ describes the internal dynamics of the system whereas $\boldsymbol{\xi}_1^*$ and $\boldsymbol{\xi}_2^*$ describe the external dynamics. The required derivatives of the outputs y_1 and y_2 can be calculated by applying the Lie-derivative (Isidori, 1995)

$$L_{\mathbf{f}}\mathbf{h}(\mathbf{x}^*) = \frac{\partial\, \mathbf{h}(\mathbf{x}^*)}{\partial \mathbf{x}^*}\mathbf{f}(\mathbf{x}^*) \tag{10}$$

to (Eq. 7). The equations for $\boldsymbol{\eta}$ can in general be chosen freely as long as the resulting transformation $\boldsymbol{\Phi}$ is a diffeomorphism. In this case

$$\eta_1^* = \dot{\psi}^* \tag{11a}$$

$$\eta_2^* = \psi_t^* \tag{11b}$$

are chosen. To obtain $\mathbf{x}^*$ the reverse coordinate transformation can be used

$$\mathbf{x}^* = \boldsymbol{\Phi}^{-1}(\mathbf{z}^*). \tag{12}$$

As can be seen, from (Eq. 9), $\boldsymbol{\xi}_1^*$ and $\boldsymbol{\xi}_2^*$ can directly be obtained from the desired trajectory whereas the states of the internal dynamic η^* are not directly available. Therefore, in a first step derivatives of the internal dynamics are calculated using (Eq. 7):

$$\dot{\eta}_1^* = \ddot{\psi}^* = q_1(\boldsymbol{\xi}_1^*, \boldsymbol{\xi}_2^*, \boldsymbol{\eta}^*) \tag{13}$$

$$\dot{\eta}_2^* = \dot{\psi_t}^* = q_2(\boldsymbol{\xi}_1^*, \boldsymbol{\xi}_2^*, \boldsymbol{\eta}^*). \tag{14}$$

Starting at the initial system state $\mathbf{x}^*(\mathbf{0}) = \mathbf{x}_\mathbf{0}^*$ the internal dynamics η^* can be obtained through integration and, thus, $\mathbf{x}^*$ can be retrieved by (Eq. 12). Finally the inversion-based feedforward control can be calculated by putting $\mathbf{x}^*$ into the Hirschorn Inverse:

$$\mathbf{u}_{\text{ff}}^* = \begin{bmatrix} L_{\mathbf{g}_1} L_{\mathbf{f}}^2 h_1(\mathbf{x}^*) & L_{\mathbf{g}_2} L_{\mathbf{f}}^2 h_1(\mathbf{x}^*) \\ L_{\mathbf{g}_1} L_{\mathbf{f}}^3 h_2(\mathbf{x}^*) & L_{\mathbf{g}_2} L_{\mathbf{f}}^3 h_2(\mathbf{x}^*) \end{bmatrix}^{-1} \begin{bmatrix} \dddot{y}_1^* - L_{\mathbf{f}}^3 h_1(\mathbf{x}^*) \\ {}^{(4)}y_2^* - L_{\mathbf{f}}^4 h_2(\mathbf{x}^*) \end{bmatrix}. \tag{15}$$

For simplicity, the dependence of the Hirschorn Inverse from the time-variant curvature is not illustrated here. The complete feedforward structure is illustrated in Fig. 3.

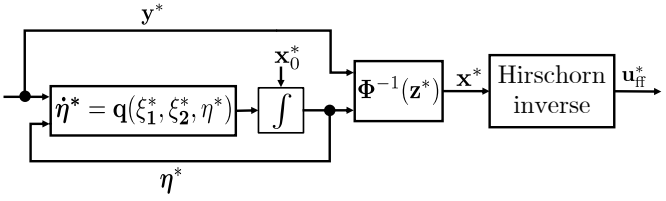

Fig. 3. Structure of the inversion-based feedforward control

3.2 Time-Variant Linear Quadratic Regulator

Amongst the variety of control laws for linear time-variant systems there exist two basic control concepts. The first concept is based on the transformation of the time-variant system to a time-invariant canonical form (Silverman, 1966). Having a linear time-invariant system almost any linear control concept can be applied. The second concept is to design a time-invariant linear quadratic regulator by solving a Riccati differential equation. The latter results in a much simpler control law and is, therefore, chosen in the following. The theory behind the controller design is taken from Athans and Falb (1966). To obtain the linear time-variant error dynamics

$$\boldsymbol{\Delta}\dot{\mathbf{x}} \quad = \mathbf{A}(t)\boldsymbol{\Delta}\mathbf{x} + \mathbf{B}(t)\boldsymbol{\Delta}\mathbf{u} \tag{16a}$$

$$\boldsymbol{\Delta}\mathbf{x}(0) = \boldsymbol{\Delta}\mathbf{x_0} = \mathbf{x_0} - \mathbf{x_0^*} \tag{16b}$$

$$\boldsymbol{\Delta}\mathbf{y} \quad = \mathbf{C}(t)\boldsymbol{\Delta}\mathbf{x}, \tag{16c}$$

the nonlinear system (7) is linearized along a trajectory $\mathbf{y}(t)^*$ with corresponding state $\mathbf{x}(t)^*$, control input $\mathbf{u}(t)^*$,

and initial state $\mathbf{x}_0 = \mathbf{x}_0^*$. The state matrices are obtained by Jacobian linearization

$$\mathbf{A}(t) = \left.\frac{\partial\left(\mathbf{f}(\mathbf{x}) + \mathbf{g}(\mathbf{x})\right)}{\partial\,\mathbf{x}}\right|_{\mathbf{x}(\mathbf{t})^*,\mathbf{u}(\mathbf{t})^*} \tag{17a}$$

$$\mathbf{B}(t) = \left.\frac{\partial\,\mathbf{g}(\mathbf{x})}{\partial\,\mathbf{u}}\right|_{\mathbf{x}(\mathbf{t})^*,\mathbf{u}(\mathbf{t})^*} \tag{17b}$$

$$\mathbf{C}(t) = \left.\frac{\partial\,\mathbf{h}(\mathbf{x})}{\partial\,\mathbf{x}}\right|_{\mathbf{x}(\mathbf{t})^*,\mathbf{u}(\mathbf{t})^*}. \tag{17c}$$

The time-variant system (16) describes the deviation of $\mathbf{x}$ from the desired state $\mathbf{x}^*$. The task of the controller is to keep this deviation small i.e. ideally $\boldsymbol{\Delta}\mathbf{x} = \mathbf{x} - \mathbf{x}^* = 0$. Hence, the trajectory tracking problem reduces to the state regulator problem in this case. To design an optimal state regulator a cost function of the form :

$$\begin{aligned} J(\mathbf{u}) =& \frac{1}{2}\boldsymbol{\Delta}\mathbf{x}'(t_f)\mathbf{F}\boldsymbol{\Delta}\mathbf{x}(t_f) + \cdots \\ &\cdots + \frac{1}{2}\int_{t_0}^{t_f}\left\{\boldsymbol{\Delta}\mathbf{x}'(t)\mathbf{Q}\boldsymbol{\Delta}\mathbf{x}(t) + \mathbf{u}'(t)\mathbf{R}\mathbf{u}(t)\right\}\mathrm{d}t \end{aligned} \tag{18}$$

is used. $\mathbf{F}$ and $\mathbf{Q}$ are positive semidefinite weighting matrices whereas $\mathbf{R}$ is positive definite. $t_f = t_0 + T_f$ where T_f is the prediction horizon. The weighting matrices $\mathbf{Q}$ and $\mathbf{R}$ could also be chosen to be time-variant because time-variant matrices can be advantageous. Assume the system has a huge initial error this would lead to a huge control input. To avoid huge control inputs the weighting matrices could penalize the error during a small initial time interval less severely. Nevertheless, in this work it is assumed the controller follows the trajectory precisely and therefore initial errors are small and thus the choice of constant weighting matrices is justified. The weighting matrices are given in Appendix A. The solution of the cost function (18) leads to an optimal and unique control

$$\mathbf{u}_{\mathrm{fb}}(t) = -\mathbf{K}(t)\mathbf{x}(t) = -\mathbf{R}^{-1}\mathbf{B}'(t)\mathbf{P}(t)\mathbf{x}(t) \tag{19}$$

where $\mathbf{K}(t)$ is the linear-time-variant control gain and $\mathbf{P}(t)$ is the positive definite symmetric solution of the Riccati differential equation

$$\begin{aligned} \dot{\mathbf{P}}(t) =& -\mathbf{P}(t)\mathbf{A}(t) - \mathbf{A}'(t)\mathbf{P}(t) + \cdots \\ &\cdots + \mathbf{P}(t)\mathbf{B}(t)\mathbf{R}^{-1}\mathbf{B}'(t)\mathbf{P}(t) - \mathbf{Q} \end{aligned} \tag{20a}$$

$$\mathbf{P}(t_f) = \mathbf{F}. \tag{20b}$$

As the final state of the Riccati equation is known it can be solved by integrating (20a) backward in time. The structure of the calculation of the optimal control gain is illustrated in Fig. 4.

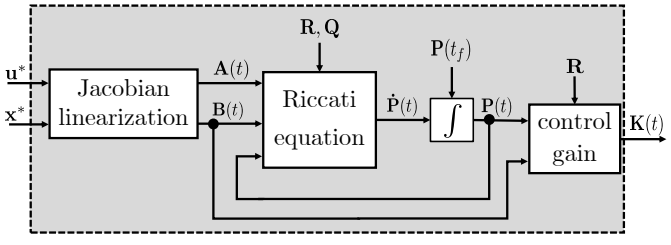

Fig. 4. Calculation of the time-variant control gain $\mathbf{K}(t)$

The controller described so far follows a given trajectory precisely. During a normal ride on the highway, a lot of times the vehicles has to keep a constant velocity over a longer period of time. In this case, the tracking problem reduces to a set point problem and thus stationary accuracy is needed. Therefore the state vector $\boldsymbol{\Delta}\mathbf{x}$ is augmented by an integral state e_v with

$$\dot{e}_v = \Delta v = v - v^*. \tag{21}$$

The integral state also compensates for disturbances e.g. air drag, wind forces, etc. which were neglected in the modeling. For the lateral direction output d an integral part is not necessary because the stationary error is small. For automated driving, the given desired trajectory has to be updated periodically to adjust to current traffic situations. The time-variant controller is based on a linearized model along a the desired trajectory $\mathbf{y}^*$. So if the trajectory changes the computed control law $\mathbf{K}(t)$ is not valid anymore and the controller needs to be updated as well. Therefore, it is necessary to periodically solve the Riccati equation (20a) online via backward integration. The replanning is done every T_c seconds. During a control horizon, n control inputs are applied to the vehicle. Thus the time-variant feedback gain needs to be evaluated at every $t_i \in \left\{0, \frac{T_c}{n}, ..., (n-1)\frac{T_c}{n}\right\}$ as depicted in Fig. 5.

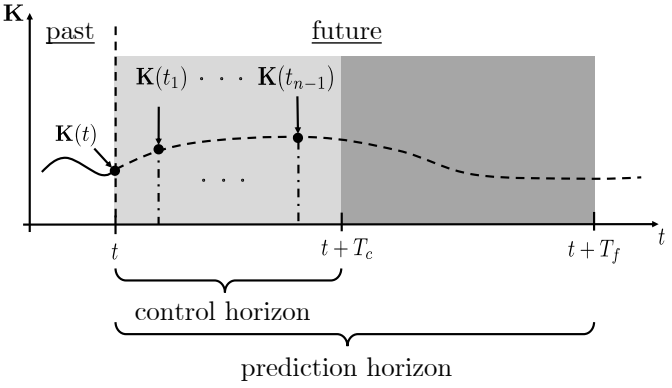

Fig. 5. Time scheme of the periodic replanning TVLQR

Due to real-time requirements, it is necessary to keep computation time small. The computation time to solve the Riccati equation (20a) only depends on the prediction horizon T_f and thus a small prediction horizon keeps the computational effort low. On the other hand the longer the prediction horizon the more future knowledge can be included in the calculation of $\mathbf{K}(t)$. So a compromise has to be made here.

4. BENCHMARK CONTROLLER

In this section a full nonlinear control concept for vehicle guidance based on feedback linearization is shortly presented as benchmark for the controller presented in the previous section. In the second part of this section the benchmark controller and the 2DOF concept are compared to each other on a conceptional level. A quantitative performance comparison is given afterwards in Section 5.

4.1 Feedback Linearization based Nonlinear Control

The benchmark controller is a feedback linearization (FL) based on an earlier work (Schucker and Konigorski, 2018)

and is only shortly summarized here. The basic structure of the control concept is illustrated in Fig. 6. The linearizing

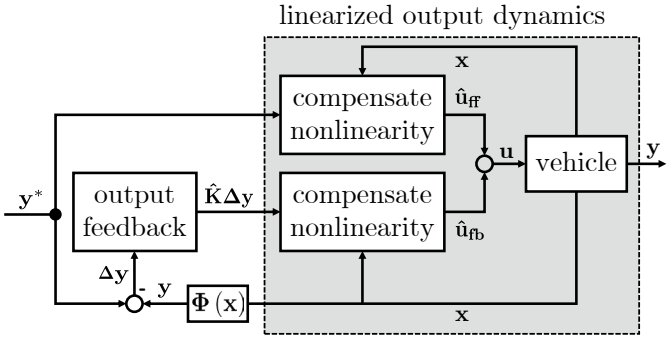

Fig. 6. Basic structure of a feedback linearization controller

feedback compensates the nonlinearities of the nonlinear vehicle model and decouples the resulting linear output dynamics so that two independent linear integrator chains are obtained (Fig. 7). Note the linear and decoupled model only describes the input to output behavior, i. e. the external dynamics of the nonlinear model. Having a linear time-invariant (LTI) model a pseudo-feedforward control and a LTI output feedback controller can be applied. The pseudo-feedforward and the feedback control laws look similar as the inversion-based feedforward control (15) and are also based on the Hirschorn Inverse:

$$\hat{\mathbf{u}}_{\mathrm{ff}} = \begin{bmatrix} L_{\mathbf{g}_1} L_{\mathbf{f}}^2 h_1(\mathbf{x}) & L_{\mathbf{g}_2} L_{\mathbf{f}}^2 h_1(\mathbf{x}) \\ L_{\mathbf{g}_1} L_{\mathbf{f}}^3 h_2(\mathbf{x}) & L_{\mathbf{g}_2} L_{\mathbf{f}}^3 h_2(\mathbf{x}) \end{bmatrix}^{-1} \begin{bmatrix} \ddot{y}_1^* - L_{\mathbf{f}}^3 h_1(\mathbf{x}) \\ \overset{(4)}{y}_2^* - L_{\mathbf{f}}^4 h_2(\mathbf{x}) \end{bmatrix} \tag{22}$$

$$\hat{\mathbf{u}}_{\mathrm{fb}} = \begin{bmatrix} L_{\mathbf{g}_1} L_{\mathbf{f}}^2 h_1(\mathbf{x}) & L_{\mathbf{g}_2} L_{\mathbf{f}}^2 h_1(\mathbf{x}) \\ L_{\mathbf{g}_1} L_{\mathbf{f}}^3 h_2(\mathbf{x}) & L_{\mathbf{g}_2} L_{\mathbf{f}}^3 h_2(\mathbf{x}) \end{bmatrix}^{-1} \left(\hat{\mathbf{K}}\Delta\mathbf{y} - \begin{bmatrix} L_{\mathbf{f}}^3 h_1(\mathbf{x}) \\ L_{\mathbf{f}}^4 h_2(\mathbf{x}) \end{bmatrix} \right) \tag{23}$$

where $\hat{\mathbf{K}}$ is the static gain of the output feedback controller.

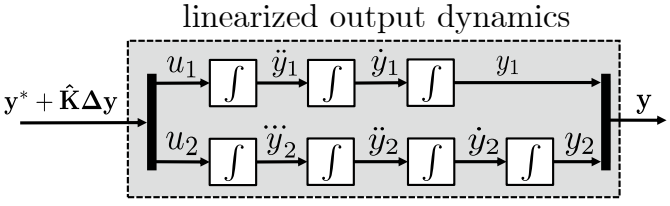

Fig. 7. Linearized and decoupled vehicle model of input/output behavior

4.2 Comparison of the Presented Control Concepts

Both of the control concepts presented in Section 3 and 4 consist of a feedforward and a feedback part. Thus, the comparison is split into these two parts.

Feedforward
Both concepts use exactly the same Hirschon Inverse to calculate the feedforward control. The only difference is that 2DOF uses the desired state $\mathbf{x}^*$ whereas FL requires the current state $\mathbf{x}$. Thus, the feedforward control of FL is only a pseudo-feedforward since it does not solely depend on desired values. This is why in Fig. 6 the term $\mathbf{u}_{\mathrm{ff}}$ does not have an asterisk. Being dependent on the current state makes the feedforward control of FL sensitive to measurement errors. If a measurement of the current state is erroneous it can happen that the Hirschorn Inverse (22) does not compensate the nonlinearities of the system any more and, hence, the complete feedforward control fails. In contrast, the feedforward control of 2DOF is not affected by measurements at all. The only requirement is that the vehicle stays close to the desired trajectory.

Feedback
Both control concepts allow a linear controller design. For TVLQR the linear time-variant model is obtained by Jacobian linearization. It represents the full state error dynamics and a linear time-variant state feedback controller is applied. Hence, the control gain $\mathbf{K}(t)$ is time-variant. In contrast, for FL the linear model is obtained by compensating the nonlinearities with a nonlinear feedback term (see Fig. 6). The result is a decoupled LTI model of the output dynamics which has a reduced order compared to the original model (7) (see Fig. 7). Thus, the resulting control gain $\hat{\mathbf{K}}$ is constant. The model reduction comes with the benefit that the number of control parameters reduces as well. The disadvantage of the model reduction is that the remaining dynamics, the internal dynamics, has to be stable. The FL controller depends on the Hirschorn Inverse and can, therefore, also be sensitive to measurement errors. A beneficial property of the FL is the decoupling of the outputs. This makes it possible to set desired dynamics for each output independently. TVLQR, in contrast, has the advantageous property of full state feedback. This allows to also penalize states and not only the outputs. Furthermore, the compensation of the nonlinearities of FL is not always the best choice because nonlinearities can, in general, also be beneficial for a controller in terms of e.g. settling time. Last but not least the control equations (22) and (23) of FL both depend on the time-variant parameter $\kappa(t)$ and the time-variant trajectory $\mathbf{y}(t)$. Thus FL actually is a nonlinear time-variant controller.

5. EXPERIMENTAL SETUP AND RESULTS

In order to give a proof of concept, simulation results as well as outcomes obtained in a prototype vehicle are presented. As mentioned before an Opel Insignia Sports Tourer as presented in Fig. 8 is used as prototype vehicle.

Fig. 8. Prototype vehicle: Opel Insignia Sports Tourer

The experimental setup is shown in Fig. 9. The intrinsic states ($\dot{\psi}, v, \delta, \dot{\delta}, F_x$ and $\dot{F}_x$) are captured with basic vehicle sensors, e. g. an inertial measurement unit. Signals obtained by a monocular camera (d and ψ_t) and signals

obtained from an observer (β) are considered as extrinsic signals.

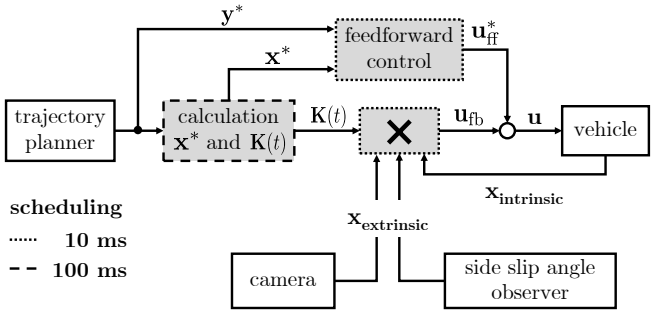

Fig. 9. Experimental setup and scheduling of the controller components (gray background)

In the following, the simulation experiment is done using a rather challenging highway scenario whereas the experimental result is performed with a slightly simpler scenario. This is due to the fact that the available test ground only offers a flat and straight road.

5.1 Simulation Results

The simulation was executed using CarMaker [1] . CarMaker provides both a detailed modeling of the vehicle as well as the whole environment (street, traffic, etc.). Since CarMaker does not provide a camera module a self made simple camera model is used.

A common highway scenario is chosen to demonstrate the capabilities of the developed control concepts. The street is a right-turning clothoid which has an initial radius of 2,500 m that reduces to 2,000 m. It also has a slight lateral slope as recommended by the highway construction guidelines. The maneuver is a lane change with a simultaneous increase of speed as it is typical for an overtaking maneuver (see Fig. 10). The lane change is done to the left and speed increases from 25 $\frac{m}{s}$ to 30 $\frac{m}{s}$. In addition, the longitudinal slope is increased stepwise by steps of 1 % (see Fig. 11) to represent a piecewise constant disturbance. The reference trajectory for the controller is calculated by a trajectory planner module which is updated every 100 ms. The desired lateral position is given, as explained in Section 2, with respect to the center of the current lane.

From Fig. 12 it can be seen that both controllers follow the desired trajectory excellently. 2DOF shows a slightly better performance in longitudinal direction whereas FL has superior behavior for the lateral direction. Furthermore, the upper plot in Fig. 12 shows the ability of the integral action in (21) to compensate constant disturbances.

5.2 Experimental Results

The scenario performed for the experimental result is a simplified version of the scenario presented in Section 5.1. Specifically, this means the road is straight and the longitudinal slope is zero and thus it reduces to a basic overtaking maneuver. Experimental results are illustrated in Fig.

[1] https://ipg-automotive.com/, release 5.1.4

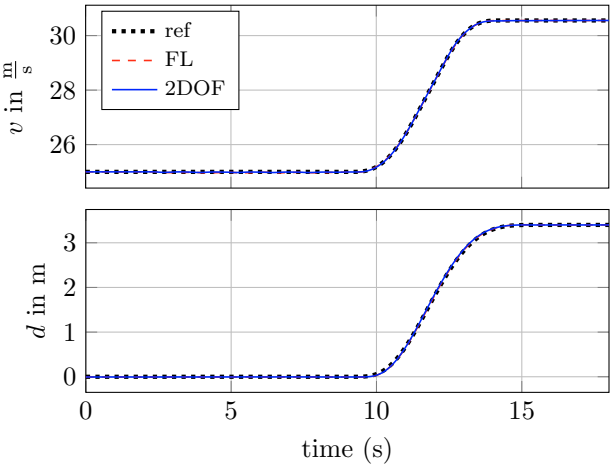

Fig. 10. Reference trajectory and tracking behavior of the control concepts for a take over maneuver

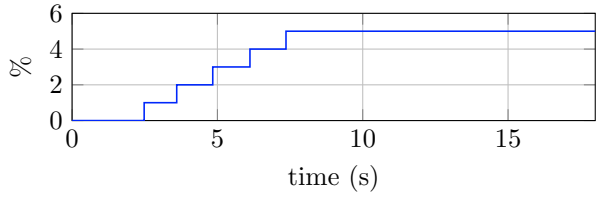

Fig. 11. Change of the longitudinal slope during the scenario

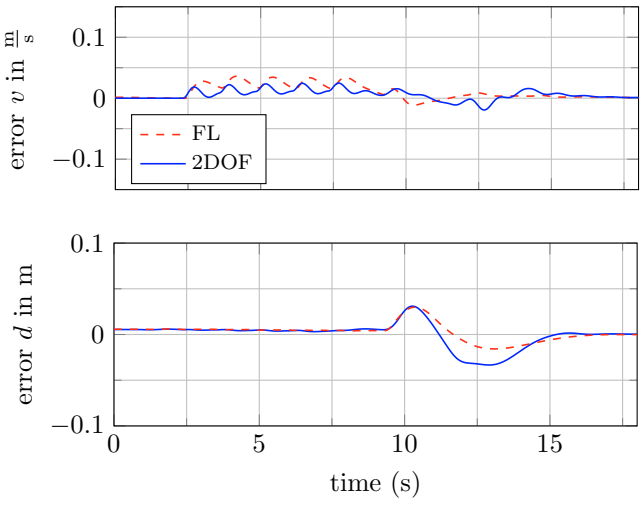

Fig. 12. Control error for a take over maneuver

13 and 14. The performance of the tracking controllers in the experimental test run confirm the simulation results. The velocity tracking of the controller is again excellent for both controllers. Though, the maximum lateral tracking error increases a bit up to roughly 0.1 m. The reason for this is assumed to be based in the subordinate steering wheel angle controller which has slight oscillating behavior even in the steady state. This oscillation seems to be reinforced by high control gains of the tracking controller.

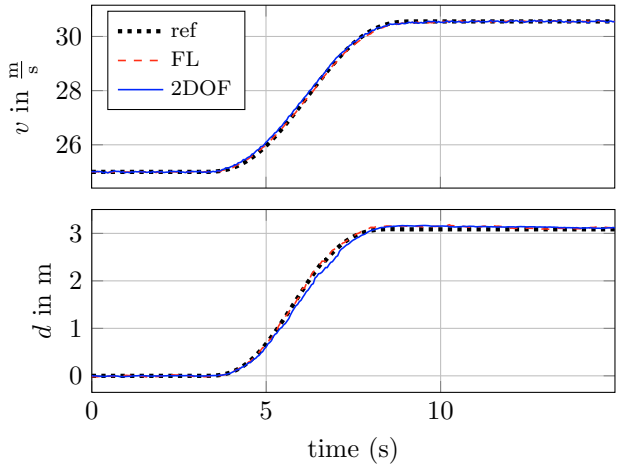

Fig. 13. Reference trajectory and tracking behavior of the control concepts for a take over maneuver

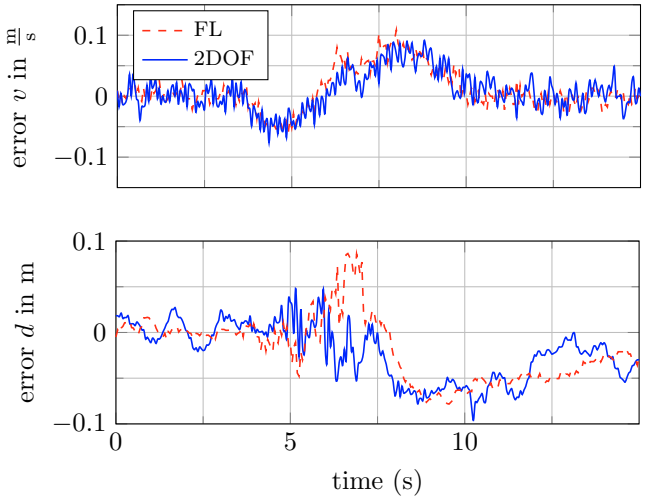

Fig. 14. Control error for a take over maneuver

6. CONCLUSION

A 2DOF control system guiding a vehicle on a given trajectory for highway scenarios was developed. The 2DOF structure consists of an inversion-based feedforward control and a time-variant linear quadratic regulator. It was shown that the presented control scheme with its simple control law can compete with a nonlinear benchmark controller in simulation as well as in the experimental results. By using a time-variant controller the presented 2DOF scheme only needs one parametrization for the whole velocity range. In addition, the 2DOF is, in general, more robust to erroneous measurements than FL. On the other hand, both feedforward controls use the same complex control law. Thus, in a next step, a simpler feedforward control is investigated. Also it has to be further investigated what exactly causes the oscillations in the steering angle for high gains in the prototype vehicle.

REFERENCES

Athans, M. and Falb, P. L. (1966). *Optimal Control: An introduction to its theory and its applications*. Lincoln Laboratory publications. McGraw-Hill and Dover Publ, Mineola, NY.

Bahadorian, M., Eaton, R., Hesketh, T. and Savkovic, B. (2014). Robust time-varying model predictive control with application to mobile robot unmanned path tracking. *IFAC Proceedings Volumes*, 47(3), 4849–4854.

Ballesteros-Tolosana, I., Rodriguez-Ayerbe, P., Olaru, S., Deborne, R. and Pita-Gil, G. (2017). Lane centering assistance system design for large speed variation and curved roads. In *IEEE Conference on Control Technology and Applications (CCTA)*, 267–273.

Freund, E. and Mayr, R. (1997). Nonlinear path control in automated vehicle guidance. *IEEE transactions on robotics and automation*, 13(1), 49–60.

Hirschorn, R. M. (1979). Invertibility of nonlinear control systems. *SIAM Journal on Control and Optimization*, 17(2), 289–297.

Horowitz, I. M. (1963). *Synthesis of Feedback Systems*. Elsevier Science, Burlington.

Isidori, A. (1995). *Nonlinear control systems*. Communications and control engineering series. Springer, London, 3rd edition.

Miah, S., Farkas, P. A., Gueaieb, W., Chaoui, H. and Hossain, M.A. (2017). Linear time-varying feedback law for vehicles with ackermann steering. *International Journal of Robotics and Automation*, 32(1).

Rajamani, R. (2012). *Vehicle dynamics and control*. Mechanical engineering series. Springer, New York, 2nd edition.

Riekert, P. and Schunk, T. E. (1940). Zur Fahrdynamik des Gummibereiften Kraftfahrzeugs. *Ingenieur Archiv*, 11.

Schorn, M. and Isermann, R. (2006). Automatic steering and braking for a collision avoiding vehicle. *IFAC Proceedings Volumes*, 39(16), 378–383.

Schucker, J. and Konigorski, U. (2018). Nonlinear vehicle trajectory guidance for automated driving on highways. In *Proceedings of IFAC Symposium on Robotic Control*.

Silverman, L. (1966). Transformation of time-variable systems to canonical (phase-variable) form. *IEEE transactions on Automatic Control*, 11(2), 300–303.

Thimmaraya, R., Nataraj, C. and Lee, D. (2010). Linear time-varying tracking control with application to unmanned aerial vehicles. In *American Control Conference (ACC)*, 806–811.

Werling, M., Gröll, L. and Bretthauer, G. (2010). Invariant trajectory tracking with a full-size autonomous road vehicle. *IEEE Transactions on Robotics*, 26(4), 758–765.

Appendix A. 2DOF WEIGHTING MATRICES

The weighting matrices are chosen to be diagonal. This makes the parametrization simpler since every parameter only penalizes one state. The weighting matrices are

$$\mathbf{Q} = \mathrm{diag}(k_{e_v},\, k_d,\, k_{\psi_t},\, k_{\dot{\psi}},\, 0,\, k_v,\, 0,\, 0,\, 0,\, 0) \tag{A.1a}$$

$$\mathbf{R} = \mathrm{diag}(k_{\delta_c},\, k_{F_{x,c}}) \tag{A.1b}$$

with $k_i,\ i \in [e_v,\, d,\, \psi_t,\, \dot{\psi},\, \delta_c,\, F_{x,c}]$ being the weighting factor for each state. A zero entry means that the state is not weighted. The quantities e_v, v, d, δ_c and $F_{x,c}$ are penalized for obvious reason since they represent the tracking outputs and the control inputs respectively. The penalization of the yaw angles $\dot{\psi}$ and ψ_t helps to reduce unnecessary steering movements.